Texture of Superfluid ^{3}He Probed by a Wigner Solid

Hiroki Ikegami* and Kimitoshi Kono

Low Temperature Physics Laboratory, RIKEN, Hirosawa 2-1, Wako, Saitama, 351-0198, Japan

(Received 26 July 2006; published 20 October 2006)

The resistivity of the Wigner solid floating on the free surface of superfluid ^{3}He has been measured in both the A and B phases down to 200 μK in the magnetic field. The resistivity in the A phase shows the asymptotic behavior to the temperature-square dependence at low temperatures. The temperature dependence is successfully explained by the uniform $\hat{\boldsymbol{l}}$ texture oriented normal to the surface and by the specular scattering of quasiparticles excited along $\hat{\boldsymbol{l}}$ vector. In the B phase, the resistivity exhibits the exponential decrease at low temperatures. The steep increase of the resistivity observed at high magnetic field is attributable to the nonuniform texture of the field-distorted order parameter induced near the surface.

DOI: 10.1103/PhysRevLett.97.165303 PACS numbers: 67.57.−z, 73.20.−r

Superfluid ^{3}He with p-wave pairing is the best understood anisotropic superfluid or superconductor [1]. Its rich structure of the order parameter gives rise to a large number of possible superfluid states with different symmetries. The isotropic phase called the B phase appears only in the zero magnetic field. In the magnetic field, the order parameter of the B phase is distorted ellipsoidally and superfluid properties become anisotropic. Application of the strong field over about 0.3 Tesla causes the phase transition into the A phase, which has an anisotropic energy gap with nodes along $\hat{\boldsymbol{l}}$ vector (see phase diagram in Fig. 4 inset)

One of the peculiar features of anisotropic superfluids is high sensitivity to boundary scattering. Free surface of superfluid ^{3}He is a very unique boundary which reflects quasiparticles (QPs) in a specular way. The specular reflection enhances the anisotropy of the order parameter [2,3] and induces several intriguing phenomena. The Andreev reflection (AR) and the Andreev bound state are expected within the coherence length (~100 nm) from the surface [2,3]. A novel surface state with different symmetry is predicted [4]. For much longer length scale, the free surface induces spatial variation of the anisotropic order parameter called texture when it is combined with other orientation effects such as magnetic field. All of the above mentioned phenomena strongly affect the dynamics of ballistic QPs, and therefore QP detection at the surface provides us valuable information about them.

A two-dimensional electron solid [the Wigner solid (WS)] realized on the free surface is a unique and sensitive detector for QPs arriving at the free surface [5,6]. In this Letter, we present new extensive measurements of the resistivity of the WS in both the A and B phases down to 200 μK in magnetic field applied parallel to the surface. We found the resistivity is strongly affected by the orientation of the order parameter near the surface in both phases.

The electrons on the helium surface crystallize into the WS at low temperatures, which accompanies periodic deformation of the surface (dimple lattice) under the lattice-localized electrons [7,8]. Owing to the dimple lattice, low-frequency transport of the WS is strongly affected by properties of the underlying liquid. In the long mean-free path regime below about 20 mK, the resistivity of the WS is dominated by specular scattering of ballistic QPs by the dimple lattice (see Fig. 1) [6]. On the scattering process, they transfer their momenta to the dimple lattice, causing the drag force to the motion of the WS. The resistivity R of the WS is described as [6,9]

$$R/R_c = \sum_{\sigma} \langle (\exp[\Delta_{\hat{\boldsymbol{k}},\sigma}(T)/k_B T] + 1)^{-1} \rangle, \qquad (1)$$

where R_c is the resistivity at the superfluid transition temperature T_c (= 0.93 mK), k_B is the Boltzmann constant, and $\Delta_{\hat{\boldsymbol{k}},\sigma}(T)$ is the excitation gap of a QP with spin σ. A unit vector $\hat{\boldsymbol{k}}$ denotes the direction of the QP momentum. The angular average $\langle \cdots \rangle$ is defined by

$$\langle \cdots \rangle = \frac{2}{\pi} \int_0^{2\pi} d\phi \int_0^{\pi/2} d\theta \sin\theta \cos^3\theta \cdots, \qquad (2)$$

where θ and ϕ are polar and azimuthal angles of $\hat{\boldsymbol{k}}$ with respect to surface normal. (The WS-induced flow velocity beneath the surface is about 10^{-3} smaller than the velocity of the WS. Thus, the AR caused by this superflow field considered in Ref. [10] is negligible.) Equation (1) suggests the resistivity is sensitive to angular distribution of incident QPs. In the B phase in zero magnetic field, the observed exponential temperature dependence of the resistivity [5] reflects the isotropic excitation of QPs [6]. In the A phase, the measurements have so far been limited

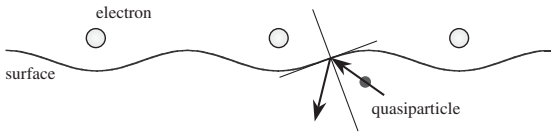

FIG. 1. Schematic drawing of specular reflection of a QP by the dimple. The spacing between electrons is approximately 1 μm, while the depth of the dimple is smaller than 0.1 nm.

only near the transition temperature [11], and low temperature behavior has not been unveiled before.

The experimental cell is shown schematically in Fig. 2(a). Liquid ^{3}He fills the bottom half of the cell. A rectangular electrode (lower electrode) is immersed into the liquid 1 mm below the surface, which is divided into two segments by a 0.2 mm gap [Fig. 2(b)]. An upper rectangular electrode is located 2 mm above the lower electrode. These two electrodes are surrounded by a rectangular guard ring made of silver. Electrons are generated at 600 mK by thermionic emission of a tungsten filament and trapped on the surface by applying positive dc voltage to the lower electrode. The electron density n_s is determined by the saturation condition. The resistivity is measured with the capacitive method. A 100 kHz ac voltage with an amplitude of 2 $mV_{p\text{-}p}$ is superimposed on one segment of the lower electrode. The induced current flowing in the surface state electron is detected by the another segment. The data shown here are taken at $n_s = 1.2 \times 10^{12}$ m^{-2} corresponding a melting temperature of the WS of 230 mK, and at the holding electric field 2.80×10^4 V/m.

The magnetic field B is applied parallel to the electric current to avoid a cyclotron motion of the electrons. The homogeneity of the field is better than 10^{-2} over the electrode. The liquid ^{3}He is cooled down to 200 μK in the magnetic field by a specially designed heat exchanger with a surface area of 142 m^2. To determine the temperature T of the liquid directly, we employ, below 450 μK, a vibrating wire resonator 12 μm in diameter installed at the end of the cell, where the B phase is always realized in the small stray magnetic field ($<$70 mT). At higher temperatures, a platinum NMR thermometer mounted on a nuclear stage is employed. The data are taken by sweeping the temperature with 10–30 μK/h.

In normal phase, the measured R is proportional to T^{-2} above 20 mK and tends to be constant below 20 mK, which

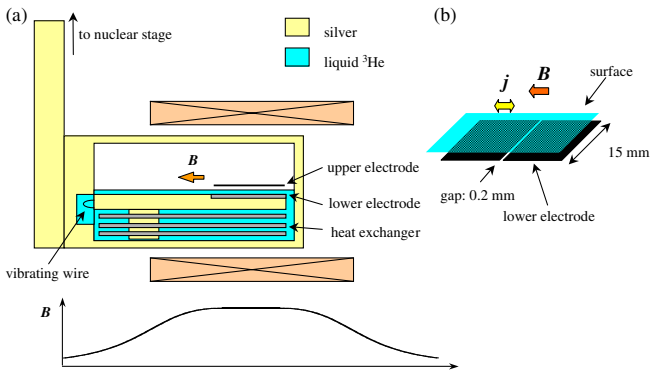

FIG. 2 (color online). (a) Schematic picture of the experimental cell and the profile of the magnetic field. (b) Lower electrode. The ac electric current (j) is induced in the direction perpendicular to the gap. The magnetic field is applied parallel to the electric current.

are consistent with the previous results [9,12]. No magnetic field dependence is observed at any temperatures in normal phase, proving that change of properties of the electrons due to the field is negligible and that the magnetic field is in parallel with the electric current enough not to cause cyclotron motion of electrons.

Figure 3 shows the temperature dependence of R of the WS on the superfluid at 0.363 Tesla, where the A phase is stable down to zero temperature. In the figure, R is normalized by the value R_c ($=2.7 \times 10^7$ Ω) at T_c. With decreasing T, R suddenly starts to decrease at T_c. R in the A phase is considerably higher than that in the B phase (see Fig. 4), reflecting the high density of QPs excited in the nodal direction.

The gap of the ABM state is expressed as $\Delta_{\hat{k},\sigma}(T) = \Delta_A(T)\sin\psi$, where ψ is the polar angle of $\hat{k}$ from $\hat{l}$. The approximate temperature dependence of $\Delta_A(T)$ is given by [13]

$$\Delta_A(T) = 2.03 k_B T_c \tanh[1.69(T_c/T - 1)^{1/2}]. \quad (3)$$

In our experimental configuration, the $\hat{l}$ texture aligned uniformly normal to the surface is most stable because the $\hat{l}$ vector prefers to be oriented normal to the surface and perpendicular to the magnetic field. The calculated resistivity for this $\hat{l}$ texture quantitatively reproduces the experimental data as shown in Fig. 3. Note there are no adjustable parameters here. In the figure, another simple case, where the $\hat{l}$ vector is uniformly aligned parallel to the magnetic field, is included for comparison. The agreement to the former case indicates that the uniform $\hat{l}$ texture normal to the surface is realized at least near the surface. It should be noted that neither the AR nor the Andreev

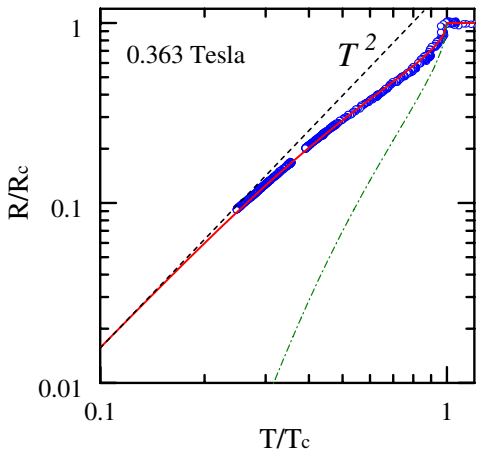

FIG. 3 (color online). Resistivity at 0.363 Tesla, corresponding to the A phase, as a function of T/T_c. The solid line is the theoretical curve when the $\hat{l}$ vector uniformly aligns normal to the surface (see text). The dash-dotted line is that for the uniform $\hat{l}$ texture aligning parallel to the field. The dashed line is the T^2 dependence.

bound state at the free surface is expected in this $\hat{\boldsymbol{l}}$ texture [2,3].

The most remarkable feature is the asymptotic behavior to the T^2 dependence at low temperatures. It reflects the linear increase of the A phase gap with ψ near the nodes, and moreover strongly suggests no admixture of other symmetries to the pure ABM state even at lowest temperatures, being consistent with the thermodynamic measurement [14]. To our knowledge, this is the first observation of the power-law behavior in mechanical response at such low temperatures. The key factor for our observation is good control of the $\hat{\boldsymbol{l}}$ texture by the free surface and the magnetic field.

Now we turn to the results of the B phase. R at several fields is shown in Fig. 4. With decreasing T, R drops suddenly at T_c and follows the theoretical curve of the A phase. Then, sharp jumps corresponding to the AB transition are observed. The AB transition shows no hysteretic behavior on cooling and warming. Below the AB transition, R exhibits the exponential temperature dependence. Moreover, R shows apparent increase with the magnetic field. The increase is attributable to the change in property of the B phase, since no field dependence is found in the normal phase as well as in the A phase. Isotherms of R at $T_c/T = 3.0$ and 3.8 are shown in Fig. 5(a) as a function of the field. R has small field dependence at low fields, but increase steeply above 0.2 Tesla.

In zero field, the B phase has the isotropic BW gap [13]

$$\Delta_B^0(T) = 1.76 k_B T_c \tanh[1.74(T_c/T - 1)^{1/2}]. \quad (4)$$

The calculated R with this gap is shown in Fig. 4. It agrees with the data at 0.070 Tesla very well.

At the free surface, part of impinging QPs are reflected with the AR [2,3], and such reflection was experimentally

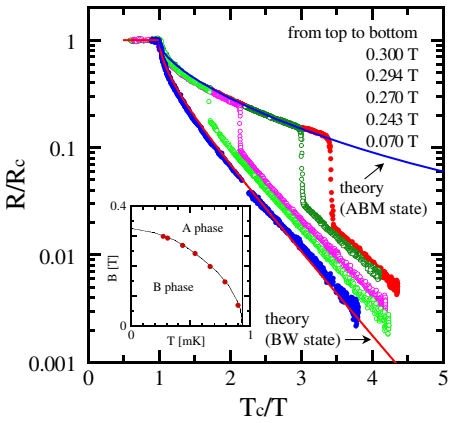

FIG. 4 (color online). Resistivity at several magnetic fields as a function of T_c/T. The vertical jumps correspond to the AB transition. The blue and red lines are the theoretical curves of the ABM state and the isotropic BW state, respectively (see text). Inset: phase diagram of superfluid ^{3}He at zero pressure obtained in this experiment.

observed [15]. On this scattering, the QP does not transfer its momentum to the dimple lattice, giving rise to reduction of R. However, the above theory [Eq. (1)] does not include the AR. Nagato *et al.* calculated the AR rate using the quasiclassical theory [3]. We estimate the effect of the AR by averaging the rate with Eq. (2). It gives only about 5% reduction of R, suggesting it is not so sensitive to the AR. However, it is possibly detected at much lower temperatures since the AR rate approaches 100% as the QP energy approaches to Δ_B^0.

Near the surface, the Andreev bound states are expected to be formed [3]. Although the Andreev bound states are considered to drag the motion of the dimple lattice, we have no theory to describe coupling between the Andreev bound states and the dimple lattice.

Next, let us consider the increase of R in high magnetic field. The strong magnetic field distorts the BW state order parameter ellipsoidally and causes, combined with the surface orientation effect, spatial variation of the order parameter. We take a triad $(\boldsymbol{e_x}, \boldsymbol{e_y}, \boldsymbol{e_z})$ as shown in Fig. 5(b); the x axis is parallel to the surface normal $\hat{\boldsymbol{s}}$ and the z axis is along to the field. In the figure, a unit vector $\hat{\boldsymbol{B}}$ denotes the direction of the field. The order parameter $\boldsymbol{d}$ of the distorted BW state is expressed as

$$\boldsymbol{d} = \begin{pmatrix} d_x \\ d_y \\ d_z \end{pmatrix} = \begin{pmatrix} \Delta_1 & & \\ & \Delta_1 & \\ & & \Delta_2 \end{pmatrix} R(\hat{\boldsymbol{n}}, \theta_L)\hat{\boldsymbol{k}}, \quad (5)$$

where $R(\hat{\boldsymbol{n}}, \theta_L)$ is a rotation matrix with a rotation angle θ_L

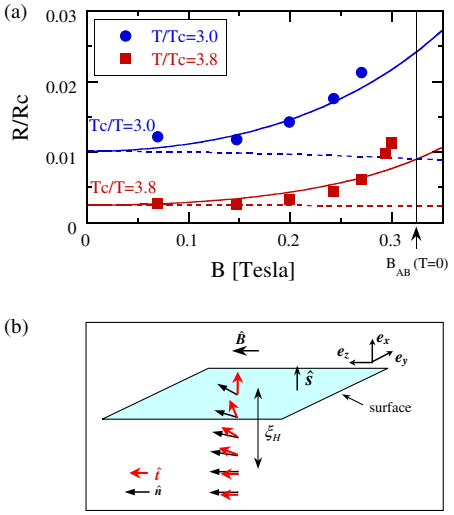

FIG. 5 (color online). (a) Isotherms of the resistivity at $T_c/T = 3.0$ and 3.8 as a function of magnetic field. The blue and red solid lines are the theoretical curves for $\hat{\boldsymbol{t}} \parallel \hat{\boldsymbol{s}}$ at $T_c/T = 3.0$ and 3.8, respectively. The dashed lines are those for $\hat{\boldsymbol{t}} \parallel \hat{\boldsymbol{B}}$. (b) Texture induced near the free surface. The black and red arrows indicate the $\hat{\boldsymbol{n}}$ and the $\hat{\boldsymbol{t}}$ vectors, respectively. In the bulk, the $\hat{\boldsymbol{t}}$ vector is oriented parallel to the field. As approaching to the surface, its direction gradually changes, and finally, it becomes normal to the surface.

around $\hat{\boldsymbol{n}}$. In the field, the energy of QP with up (+) and down (−) spin is given by [16]

$$E^2_{\hat{\boldsymbol{k}},\pm} = d_x^2 + d_y^2 + [(\xi_k^2 + d_z^2)^{1/2} \mp \hbar\tilde{\omega}_L/2]^2, \quad (6)$$

where $\hbar$ is the Plank constant and $\tilde{\omega}_L$ is the Fermi-liquid corrected-Larmor frequency which is proportional to B. ξ_k is the kinetic energy of the QP measured from the Fermi surface. The excitation gap $\Delta_{\hat{\boldsymbol{k}},\pm}$ is obtained from Eq. (6) by putting $\xi_k = 0$ and by introducing $\hat{\boldsymbol{t}} \equiv R(\hat{\boldsymbol{n}}, \theta_L)^{-1}\boldsymbol{e}_z$ and $\eta \equiv \cos^{-1}(\hat{\boldsymbol{t}} \cdot \hat{\boldsymbol{k}})$ as

$$\Delta^2_{\hat{\boldsymbol{k}},\pm} = \Delta_1^2 \sin^2\eta + (\Delta_2|\cos\eta| \mp \hbar\tilde{\omega}_L/2)^2. \quad (7)$$

It is obvious that $\Delta_{\hat{\boldsymbol{k}},\pm}$ has rotational symmetry around $\hat{\boldsymbol{t}}$.

In the bulk, $\hat{\boldsymbol{n}}$ and $\hat{\boldsymbol{t}}$ are parallel to the field due to the bulk field energy [17]. On the other hand, at the surface, $\hat{\boldsymbol{n}}$ is oriented in such a way to minimize the surface field energy which originates from the anisotropic suppression of the order parameter near the surface. The minimum can be achieved when $R(\hat{\boldsymbol{n}}, \theta_L)\hat{\boldsymbol{s}} = \pm\hat{\boldsymbol{B}}$, i.e., $\hat{\boldsymbol{t}} = \pm\hat{\boldsymbol{s}}$ [18,19], indicating the distortion axis $\hat{\boldsymbol{t}}$ is normal to the surface at the free surface. This orientation is connected to the bulk orientation by gradually changing the direction over the bending length ξ_H [Fig. 5(b)]. ξ_H is about $\frac{10}{B(\text{Tesla})}\,\mu$m in the low field region ($\hbar\tilde{\omega}_L \ll \Delta_B^0$) [17], which is much longer than the coherence length. This texture has been extensively used to interpret the NMR experiments, although the surface is the diffusive wall in most cases.

Now we can calculate the resistivity caused by this texture. The QP density arriving at the surface is dominated by the gap just below the surface. Consequently, we consider the case of $\hat{\boldsymbol{t}} \parallel \hat{\boldsymbol{s}}$ to calculate R with Eq. (1). We assume the gap is well developed to the zero temperature value. The field dependence of the gap at zero temperature including up to the order of B^2 is [16]

$$\begin{aligned} \Delta_1^2 &= \Delta_B^0(0)^2 + (\hbar\tilde{\omega}_L)^2/4; \\ \Delta_2^2 &= \Delta_B^0(0)^2 - (\hbar\tilde{\omega}_L)^2/2. \end{aligned} \quad (8)$$

At zero temperature $\tilde{\omega}_L = \gamma B(1 + \frac{1}{5}F_2^a)/(1 + \frac{2}{3}F_0^a + \frac{1}{15}F_2^a)$, where γ is the gyromagnetic ratio of ^{3}He [20]. We take the Landau parameters as $F_0^a = -0.70$ and $F_2^a = +1.04$ [21]. The calculated field dependence of R from Eq. (1) is compared with the data in Fig. 5(a). The agreement is satisfactory. We note there are no fitting parameters in the theoretical curves. The small discrepancy around 0.3 Tesla is probably due to the higher order terms of B neglected in Eq. (8) or remaining temperature dependence of the gap. In Fig. 5(a), the resistivity isotherms in case that the bulk orientation persists up to the surface ($\hat{\boldsymbol{t}} \parallel \hat{\boldsymbol{B}}$) are included. These isotherms do not reproduce the data, indicating the importance of the orientation of the order parameter.

To conclude, we emphasize that the resistivity of the Wigner solid is a powerful probe to investigate the texture formed under the free surface. Our resistivity measurements down to 200 μK prove that, in the A phase, the uniform $\hat{\boldsymbol{l}}$ texture oriented normal to the surface is realized near the surface. In the B phase, the nonuniform texture of the field-distorted order parameter induced by the combination of the free surface and the strong magnetic field significantly influences the resistivity.

We thank Y. Nagato, K. Nagai, and H. Akimoto for stimulating discussions. This work is partly supported by the Grant-in-Aid for Scientific Research from the Ministry of Education, Culture, Sports, Science, and Technology of Japan.

*Electronic address: hikegami@riken.jp

[1] D. Vollhardt and P. Wölfle, *The Superfluid Phases of Helium 3* (Taylor & Francis, London, 1990).
[2] W. Zhang, J. Kurkijärvi, D. Rainer, and E. V. Thuneberg, Phys. Rev. B **37**, 3336 (1988).
[3] Y. Nagato, M. Yamamoto, and K. Nagai, J. Low Temp. Phys. **110**, 1135 (1998).
[4] E. V. Thuneberg, Phys. Rev. B **33**, 5124 (1986).
[5] K. Shirahama, O. I. Kirichek, and K. Kono, Phys. Rev. Lett. **79**, 4218 (1997).
[6] Y. P. Monarkha and K. Kono, J. Phys. Soc. Jpn. **66**, 3901 (1997).
[7] *Two-Dimensional Electron Systems on Helium and Other Cryogenic Sub- strates*, edited by E. Y. Andrei (Kluwer, Dordrecht, 1997).
[8] Y. P. Monarkha and K. Kono, *Two-Dimensional Coulomb Liquids and Solids* (Springer-Verlag, Berlin, 2004).
[9] K. Kono, Physica (Amsterdam) **280B**, 112 (2000).
[10] S. N. Fisher, G. R. Pickett, and R. J. Watts-Tobin, J. Low Temp. Phys. **83**, 225 (1991).
[11] K. Shirahama, H. Suto, O. I. Kirichek, and K. Kono, Physica (Amsterdam) **284–288B**, 277 (2000).
[12] H. Suto, K. Shirahama, and K. Kono, Czech. J. Phys. Suppl. S1 **46**, 341 (1996).
[13] *Helium Three*, edited by W. P. Halperin and L. P. Pitaevskii (North-Holland, Amsterdam, 1990), Chap. 7.
[14] M. Bartkowiak, S. W. J. Daley, S. N. Fisher, A. M. Gúenault, G. N. Plenderleith, R. P. Haley, G. R. Pickett, and P. Skyba, Phys. Rev. Lett. **83**, 3462 (1999).
[15] T. Okuda, H. Ikegami, H. Akimoto, and H. Ishimoto, Phys. Rev. Lett. **80**, 2857 (1998).
[16] L. Tewordt and N. Schopohl, J. Low Temp. Phys. **37**, 421 (1979).
[17] E. V. Thuneberg, J. Low Temp. Phys. **122**, 657 (2001).
[18] H. Smith, W. F. Brinkman, and S. Engelsberg, Phys. Rev. B **15**, 199 (1977).
[19] Page 424 in Ref. [13].
[20] J. A. Sauls and J. W. Serene, Phys. Rev. Lett. **49**, 1183 (1982).
[21] R. S. Fishman and J. A. Sauls, Phys. Rev. B **38**, 2526 (1988).